Journal of Theoretical Biology ▮ (▮▮▮▮) ▮▮▮–▮▮▮

Contents lists available at ScienceDirect

Journal of Theoretical Biology

journal homepage: www.elsevier.com/locate/yjtbi

The impact of adhesion on cellular invasion processes in cancer and development

Kevin J. Painter *, Nicola J. Armstrong, Jonathan A. Sherratt

Department of Mathematics and the Maxwell Institute for Mathematical Sciences, School of Mathematical and Computer Sciences, Heriot-Watt University, Edinburgh EH14 4AS, UK

ARTICLE INFO

Article history:
Received 12 January 2010
Received in revised form
19 March 2010
Accepted 20 March 2010

Keywords:
Cancer invasion
Cell adhesion
Mathematical model
Pattern formation
Integrodifferential equation

ABSTRACT

In this paper we consider a simple continuous model to describe cell invasion, incorporating the effects of both cell–cell adhesion and cell–matrix adhesion, along with cell growth and proteolysis by cells of the surrounding extracellular matrix (ECM). We demonstrate that the model is capable of supporting both noninvasive and invasive tumour growth according to the relative strength of cell–cell to cell–matrix adhesion. Specifically, for sufficiently strong cell–matrix adhesion and/or sufficiently weak cell–cell adhesion, degradation of the surrounding ECM accompanied by cell–matrix adhesion pulls the cells into the surrounding ECM. We investigate the criticality of matrix heterogeneity on shaping invasion, demonstrating that a highly heterogeneous ECM can result in a "fingering" of the invasive front, echoing observations in real-life invasion processes ranging from malignant tumour growth to neural crest migration during embryonic development.

1. Introduction

The adhesive attachments that link cells to their surroundings are fundamental in forming and maintaining the structure and function of tissues. Correspondingly, perturbations to their normal behaviour can lead to a wide variety of pathologies, ranging from heart defects to neurological disorders. Cellular adhesion is classified into two principle forms, *cell–cell adhesion* and *cell–matrix adhesion*, the former defining the direct binding between cells, and the latter the attachment of cells to the surrounding ECM (Steinberg, 2007). Control of adhesion and, in turn, cell positioning, is determined by the expression of various transmembrane molecules, the cell adhesion molecules (CAMs), which allow communication between extracellular and intracellular signalling pathways. Cell–cell adhesion is typically mediated by the cadherin family of CAMs (Cavallaro and Christofori, 2004), the prototype being the epithelial cell–cell adhesion molecule E-cadherin, which zips cells together through a protein–protein coupling of extracellular domains. Cell–matrix adhesion is mainly regulated via the integrins, the extracellular domains of which anchor to ligands in the ECM (Berrier and Yamada, 2007).

Cell invasion occurs in a number of biological processes, notably embryonic development (for example, the wave of cell migration away from the neural crest to form, amongst others, components of the peripheral nervous system) and cancer. The transition from a noninvasive and compact tumour to an invasive one capable of generating metastases is pivotal for prognosis, and the profile of the invasive front provides a crucial diagnostic indicator: sharp and uniform fronts generally imply noninvasive tumours while diffuse and/or wavy fronts tend to indicate invasiveness. Indeed, fractal dimension algorithms have been applied to tumour boundaries to provide a quantitative measure of malignancy (Landini and Rippin, 1996; Abu-Eid and Landini, 2006).

Invasion can either occur "individually", where cells migrate as individuals to form a diffuse/indistinct tumour-host interface, or "collectively" in which groups of cells invade while maintaining tight cellular contacts (e.g. see Friedl and Wolf, 2003; Yilmaz et al., 2007; Friedl and Gilmour, 2009). Particular invasion patterns in the latter class include tumour "fingers": strands of tumour cells that project out from the main tumour mass, occasionally breaking free to form "clusters". Notably, these collective forms of invasion are characterised by the expression of both cell–cell adhesion molecules that hold cells together, and cell–matrix adhesion molecules that facilitate the invasion. Nonuniform patterns of invasion have also been observed during neural crest migration, where cells migrate out in "streams" and "chains", see for example Kulesa and Fraser (1998), Young et al. (2004), and Kasemeier-Kulesa et al. (2005).

Fundamental to many developmental instances of invasion, including neural crest migration and gastrulation, is the tightly regulated epithelial–mesenchymal transition of cells, involving a reconfiguration of their molecular repertoire such that the tight E-cadherin bonds joining it to its neighbours are dissolved while

* Corresponding author. Tel.: +44 131 4518234; fax: +44 131 4513249.
E-mail addresses: painter@ma.hw.ac.uk (K.J. Painter), nicola_j_armstrong@hotmail.com (N.J. Armstrong), jas@ma.hw.ac.uk (J.A. Sherratt).

0022-5193/$ - see front matter © 2010 Elsevier Ltd. All rights reserved.
doi:10.1016/j.jtbi.2010.03.033

various pro-migratory processes, including cell–matrix binding, matrix degradation and cellular protrusions, are upregulated. For tumours of epithelial type, progression into an invasive phenotype also shares certain elements of the epithelial–mesenchymal transition, albeit in uncontrolled fashion (see Yilmaz and Christofori, 2009 for a recent review). A drop in E-cadherin expression frequently correlates with increased tumour malignancy while forced expression of E-cadherin in cultures can reverse the invasive transformation, giving noninvasive phenotypes (e.g. see Christofori, 2003; Cavallaro and Christofori, 2004; Yilmaz and Christofori, 2009). Recent focus has been paid to a "cadherin switch" (Wheelock et al., 2008), in which loss of E-cadherin is further accompanied by gain in the mesenchymal CAM N-cadherin, and the cell subsequently loses its affinity for its epithelial neighbours.

Expansion into the surrounding environment requires interactions with the ECM, determined by the integrin family of CAMs (Berrier and Yamada, 2007). The *focal adhesions* created through integrin-ECM binding provide anchoring points, and the combination of their formation at the leading edge with detachment at the rear propels the cell forward through the matrix (e.g. Friedl and Wolf, 2009). Subsequently, the nature of the ECM plays a significant role in directing migration: cells preferentially migrate towards more adhesive (ligand dense) regions of the matrix, a process termed *haptotaxis* (Lo et al., 2000), or along the long strands of individual collagen fibres, known as *contact guidance* (Dunn and Heath, 1976; Manwaring et al., 2004).

Mesenchymal migration through the ECM also requires its structural modification via proteolytic degradation and, in addition to their mechanical role, focal adhesions provide sites for the recruitment of matrix proteases such as MMPs where they can act to cleave fibres directly to the fore of the cell, a process termed pericellular proteolysis (Friedl and Wolf, 2009). The result is tunnels through the matrix along paths of cell migration, providing potential paths of least resistance through which further expansion can take place.

While the above events—loss of cell–cell adhesion, gain in cell–matrix adhesion, proteolytic action—are often described as separate processes, the interlocking nature of cell signalling pathways inevitably precludes such simplicity. Invariably, a signalling molecule known to modify one aspect will directly impinge on another. For example, the *Snail* genes appear to play "master controller" roles with their downstream targets including a wide range of components important for invasion, including repression of E-cadherin expression and induction of various pro-migratory factors such as integrins and MMPs (e.g. Nieto, 2009). A plethora of reviews exist on the various intracellular and extracellular signalling modulators of adhesion and their role in epithelial–mesenchymal transition and tumour invasion, for example see Yilmaz and Christofori (2009).

1.1. Modelling adhesion in invasion processes

There is a significant literature on the mathematical modelling of adhesion in the context of cancer invasion. Most early work in this area involved the incorporation of adhesion via a surface tension on the tumour boundary (Byrne and Chaplain, 1996; Chaplain, 1996; Cristini et al., 2003; Frieboes et al., 2006, 2007; Friedman, 2007; Macklin and Lowengrub, 2007). This representation of adhesion is indirect: there is no explicit modelling of cell–cell or cell–matrix contact. Direct representations of adhesion were first considered in the context of individual cell-based models (Turner and Sherratt, 2002; Turner et al., 2004; Grygierzec et al., 2004). In recent years, this modelling approach has been developed significantly by Anderson and coworkers, in a series of sophisticated studies into the ways in which changes in cell–cell and cell–matrix adhesion interact with other aspects of the invasive phenotype (Anderson et al., 2006, 2009; Ramis-Conde et al., 2008; Poplawski et al., 2009).

Individual cell-based models lend themselves naturally to the inclusion of adhesive effects because cell boundaries are represented explicitly. In contrast, it is more difficult to include adhesion explicitly in continuum models. For cell–matrix adhesion Mallet and Pettet (2006) included integrins as a model variable, with cells moving up gradients of active integrin density; their work is effectively a more precise version of phenomenological models for haptotaxis (e.g. Marchant et al., 2001; Landman et al., 2008). However, this approach does not extend in any natural way to cell–cell adhesion, and it is only very recently (Gerisch and Chaplain, 2008; Kim et al., 2009; Sherratt et al., 2009) that this has been incorporated into continuum models for cancer invasion, via an integro-partial differential equation formulation that was developed initially by Armstrong et al. (2006) in the context of cell sorting, and that also forms the basis for the present study.

1.2. Outline

In this paper we develop (Section 2) a minimal model for cellular invasion within a matrix environment. We demonstrate (Section 3) its ability to predict either non-invasive or invasive growth, according to the relative strengths of cell–cell and cell–matrix adhesion, and the potentially significant role that the local ECM structure may play on the rate and form of invasion. For a "sufficiently variable" ECM environment, we show (Section 4) that the model can generate a highly variable front, similar to the various nonuniform processes of invasion described above. We conclude with a brief discussion and consider some potential future extensions.

2. Model derivation

We consider a minimal model for invasion in which a population of proliferating cells, $n(\underline{x},t)$, is deposited into an ECM environment, $m(\underline{x},t)$. It is assumed that cells form adhesive attachments both to other cells (cell–cell adhesion) and the surrounding matrix (cell–matrix adhesion), and that the force generated through this binding drives cell movement. To model these within a continuous framework we extend the integro-PDE approach developed in Armstrong et al. (2006) (see also Sekimura et al., 1999; Gerisch and Chaplain, 2008; Sherratt et al., 2009; Kim et al., 2009; Gerisch and Painter, 2010) and study the generic cell density equation

$$n(\underline{x},t)_t = \overbrace{D_n\nabla^2 n}^{\text{random motility}} \overbrace{-\nabla\cdot\left[\phi n(\underline{x},t)\int_V \frac{\underline{r}}{|\underline{r}|}\Omega(|\underline{r}|)f(n(\underline{x}+\underline{r}),m(\underline{x}+\underline{r}))\,d\underline{r}\right]}^{\text{Adhesive movement}} + \overbrace{g(\cdot)}^{\text{Cell kinetics}}. \quad (1)$$

In the above representation, $(\underline{r}/|\underline{r}|)\Omega(|\underline{r}|)f(u(\underline{x}+\underline{r}),m(\underline{x}+\underline{r}))$ defines the local force exerted on cells at $\underline{x}$ through cell–cell/cell–matrix binding at $\underline{x}+\underline{r}$, formulated through splitting it into three components:

1. the direction of the force, $\underline{r}/|\underline{r}|$;
2. the dependency of the force magnitude on the distance from $\underline{x}$, $\Omega(|\underline{r}|)$;
3. the dependency of the force magnitude on the adhesivity at $\underline{x}+\underline{r}$, $f(n(\underline{x}+\underline{r}),m(\underline{x}+\underline{r}))$.

For uniqueness we specify $\int_V \Omega(|\underline{r}|)d\underline{r} = |V|$. In practice, adhesivity undoubtedly depends on a number of factors, including the

Please cite this article as: Painter, K.J., et al., The impact of adhesion on cellular invasion processes in cancer and development. J. Theor. Biol. (2010), doi:10.1016/j.jtbi.2010.03.033

composition of receptor–receptor/receptor–ligand bindings and physical properties of the substrate. Above we simply assume that this relates to cell and matrix densities at $\underline{x}+\underline{r}$. The total force exerted at $\underline{x}$ sums all local forces over a volume V, minimally representing the mean cell volume but in practice likely to be of the order of several cell diameters due to their capacity to deform and extend protrusions. We assume that this region is symmetrical about the cell centre and take V to be either the interval $[-R,R]$ (in 1D), the circle of radius R (in 2D) or the sphere of radius R (in 3D). Herein we refer to V (R) as the sensing region (radius), since it reflects the volume over which cells can detect their neighbours. The parameter ϕ relates the force generated to movement of the cells and depends on factors such as the viscosity of the medium. The above framework can easily be extended to include additional movement cues (e.g. chemoattractants). However to focus on cell–cell and cell–matrix adhesion we ignore these, and for the same reason we shall generally assume $D_n=0$.

To describe f we adapt the choice of Armstrong et al. (2006) and consider

$$f(n,m)=(\alpha n+\beta m)[1-n/k_3-m/k_4],$$

where α and β respectively define the strengths of cell–cell and cell–matrix adhesion while the notation $[z]=\max(z,0)$. This choice reflects an approximately linear increase in force magnitude at low cell and matrix (combined) densities, and a decrease at higher densities; intuitively, the former assumes that increased densities correspond to a greater likelihood of forming bonds while the latter assumes a resistance against moving into dense regions. For $n/k_3+m/k_4=1$ the force is zero, and k_3, k_4 can be interpreted as crowding parameters. In the absence of suitable experimental data, we assume $\Omega(r)=\text{constant}(=1)$; alternative choices for Ω would be to decrease with r due to a diminished likelihood of forming bonds with distance: investigations into other forms are described in Sherratt et al. (2009).

We note that the above implies that a matrix gradient across the sampling radius can generate directional cell motility and hence describes "haptotaxis" (Lo et al., 2000). A number of previous models have represented haptotaxis through terms of the form $-\beta[nm_x]_x$ (for example, see Perumpanani et al., 1996; Chaplain and Lolas, 2005; Mallet and Pettet, 2006; Gerisch and Chaplain, 2008), however we do not consider this simplification here for two key reasons. Firstly, our model describes movement through adhesive binding and, given that cell–cell bounds are formed over some sensing radius, it is appropriate that cell–matrix bonds develop over the same range as for cell–cell adhesion. Secondly, our work will investigate model behaviour across parameter space and equivalent formulations for cell–cell and cell–matrix interactions admit direct comparison between the parameters α and β.

To describe cell growth we simply adopt a logistic growth form

$$g(n)=k_1(1-n/k_2),$$

where k_1 describes the growth rate and k_2 is the "carrying capacity". Note that the carrying capacity is considered to be distinct from the crowding parameters above: the latter describe restricted movement into highly dense tissue regions while the former defines population-limited cell growth, for example as a result of nutrient depletion or cell–cell mediated contact inhibition. It is worth noting that for a nutrient-rich environment (i.e. large k_2), the tissue density may also impact on cell growth and $g(n)$ could therefore additionally depend on the matrix density. For the present paper we ignore such scenarios: preliminary investigations with other forms for g appear to yield comparable results, but a full investigation is left for future work. Cell proliferation may also depend on cell and matrix densities across the sensing region of a cell, rather than at its centre; this possibility has been considered previously by Szymanska et al. (2009), but we neglect it here in order to focus on adhesive effects.

For many cell types, expansion and invasion of an ECM environment *in vivo* requires the dissolution of matrix to create the space into which cells can migrate (Friedl and Wolf, 2009). Invading cells produce a wide variety of proteolytic enzymes (e.g. MMPs) which are either recruited to cell–matrix adhesion sites, localising proteolysis to the cell–matrix interface (pericellular proteolysis), or secreted into the extracellular milieu where they act on matrix at a distance. In certain cases, regeneration of the ECM may also occur via the synthesis and assembly of new matrix components, but here we assume that no regeneration occurs on the timescales considered. In principle, adhesive interactions between the cells and matrix may deform the matrix structure, however we assume such effects are negligible in comparison to matrix degradation. While cell–matrix interactions have been modelled in detail by a number of authors (e.g. Chaplain and Lolas, 2005; Mallet and Pettet, 2006; MacArthur et al., 2005; Gerisch and Chaplain, 2008), our focus is on the regulation of cell-invasion through the relative levels of cell–cell and cell–matrix adhesion and we adopt the relatively simple scheme proposed by Perumpanani et al. (1996):

$$m(\underline{x},t)_t=-k_5pm, \tag{2}$$

$$p(\underline{x},t)_t=D_p\nabla^2p+k_6nm-k_7p, \tag{3}$$

where $p(\underline{x},t)$ describes the concentration of proteolytic enzymes. The model is further simplified by assuming that proteolytic secretion/action occurs directly at the cell–matrix interface (pericellular proteolysis, $D_p=0$) and that production/decay timescales for the protease are much shorter than those associated with invasion, e.g. Mignatti and Rifkin (1993). This same quasi-steady state assumption was made by Perumpanani et al. (1996) and yields $p=(k_6/k_7)nm$. In order to focus on adhesion-driven movement we set $D_n=0$, and our equations are then reduced to the cell and matrix density equations

$$n_t=\overbrace{k_1n\left(1-\frac{n}{k_2}\right)}^{\text{Proliferation}}-\overbrace{\nabla\cdot\left(\phi n\int_V\frac{\underline{r}}{|\underline{r}|}(\alpha n(\underline{x}+\underline{r})+\beta m(\underline{x}+\underline{r}))\left[1-\frac{n(\underline{x}+\underline{r})}{k_3}-\frac{m(\underline{x}+\underline{r})}{k_4}\right]d\underline{r}\right)}^{\text{Adhesive movement}}$$

$$m_t=\underbrace{-(k_5k_6/k_7)nm^2}_{\text{Proteolysis}}.$$

Substituting

$$n^*=\frac{n}{k_2},\quad m^*=\frac{k_3m}{k_2k_4},\quad t^*=k_1t,\quad \underline{x}^*=\frac{\underline{x}}{R},$$

$$\alpha^*=\frac{\alpha k_2^2\phi}{k_1k_3R},\quad \beta^*=\frac{\beta k_4k_2^2\phi}{k_1k_3^2R},\quad K=\frac{k_3}{k_2},\quad \gamma=\frac{k_5k_6k_2^2k_4}{k_1k_7k_3}$$

into the above (and dropping the *s for notational convenience) generates the nondimensional model

$$n_t=n(1-n)-\nabla\cdot\left(n\int_V\frac{\underline{r}}{|\underline{r}|}(\alpha n(\underline{x}+\underline{r})+\beta m(\underline{x}+\underline{r}))[K-n(\underline{x}+\underline{r})-m(\underline{x}+\underline{r})]\,d\underline{r}\right), \tag{4a}$$

$$m_t=-\gamma nm^2, \tag{4b}$$

where the new sensing region V is either the interval $[-1,1]$ (in 1D) or the unit circle/sphere (in 2/3D). Assuming that a cell can sense across a region of several cell diameters via elongation and

Please cite this article as: Painter, K.J., et al., The impact of adhesion on cellular invasion processes in cancer and development. J. Theor. Biol. (2010), doi:10.1016/j.jtbi.2010.03.033

protrusion, a length of 1 in the dimensionless model can be estimated as approximately 50 μm.

$n(x,t)$ and $m(x,t)$ are non-dimensional tumour cell and matrix densities at position x and time t. The parameters α, β, γ and K are henceforth referred to as the cell–cell adhesion strength (α), the cell–matrix adhesion strength (β), the matrix degradation rate (γ) and the crowding capacity (K), although we note that in reality these are non-dimensional parameters that incorporate further information. In the next sections we perform numerical simulations to investigate the potential for these parameters to impact on the rate and mode of invasion.

3. Exploration into dynamics of the invasive front

Numerous experimental studies have linked an increased tendency to invade with altered adhesive properties for various cancer cell types. In this section we explore the impact of varying ratios of adhesive coefficients in the model (4) on the cohesivity and/or infiltration of the cells.

We begin by considering a 1D geometry ($x \in [0,L]$, where $L \gg 1$, the sampling range) that describes the profile of the cell front. Our initial set-up considers a deposition of cells within a uniform matrix environment as follows:

$$n(x,0) = \begin{cases} n_0 & \text{if } x \le L_i, \\ 0 & \text{otherwise,} \end{cases} \tag{5a}$$

$$m(x,0) = m_0. \tag{5b}$$

We use reflective boundary conditions at $x=0$, corresponding to this point being the centre of an initial cell mass, with zero-flux boundary conditions at $x=L$. In practice this latter condition is of limited significance since we stop our simulations before the invasion approaches the boundary.

3.1. Impact of adhesive coefficients on invasion/non-invasion

Numerical simulations imply that the behaviour of the model is divided into two principle classes according to the sizes of β and α: for $\beta < \alpha$, "noninvasive" growth occurs, Fig. 1 (top row), in which proliferation drives cellular expansion towards the population carrying capacity, yet no expansion outside the initial deposition occurs. For $\beta > \alpha$, Fig. 1 (middle row), we observe "invasive" growth, in which the population rapidly grows and expands from its initial range to eventually fill the entire domain. Further increases in β result in faster expansion, e.g. Fig. 1 (bottom row).

Under invasive growth, cell and matrix profiles appear to evolve into formal travelling-waves (i.e. constant speed and shape) and, in Fig. 2, we calculate the wavespeed for various (α,β) pairs: while there is some dependence on the magnitudes of α and β, the rate of invasion appears to predominantly depend on the difference $\beta-\alpha$. The ability for a continuous model to exhibit non-invasive growth is unusual and can be attributed to an absence of the diffusive type terms often used to model a "random" component to cell motion. While the merits of including such terms is debatable—here our general assumption is that cells only move under the forces generated by adhesion—exploratory numerical simulations incorporating a Fickian type diffusion term indicate that solutions always generate invasive growth, regardless of the size of the diffusion coefficient. Despite this, the same general principles apply: larger cell–matrix than cell–cell adhesion generates a faster rate of invasion. We note that noninvasive growth can be generated in models including random motility of cells; it occurs via other means, for example through an ECM regrowth term, see Gerisch and Chaplain (2008).

3.2. Dependency of invasion on matrix density

The above results clearly corroborate established hypotheses on the importance of adhesion to cancer invasion: upregulated cell–matrix adhesion and/or downregulated cell–cell adhesion corresponds to a greater propensity for invasion. Similarly, migration of cells out from the neural crest requires a carefully regulated epithelial–mesenchymal transition, during which down-regulation of cell–cell adhesion is accompanied by an upregulation in cell–matrix interactions.

Intuitively, this suggests that the adhesivity/density of the matrix can play a pivotal role on the rate of invasion and we now explore this in greater detail. We first consider the impact of matrix density on the wavespeed by considering the rate of

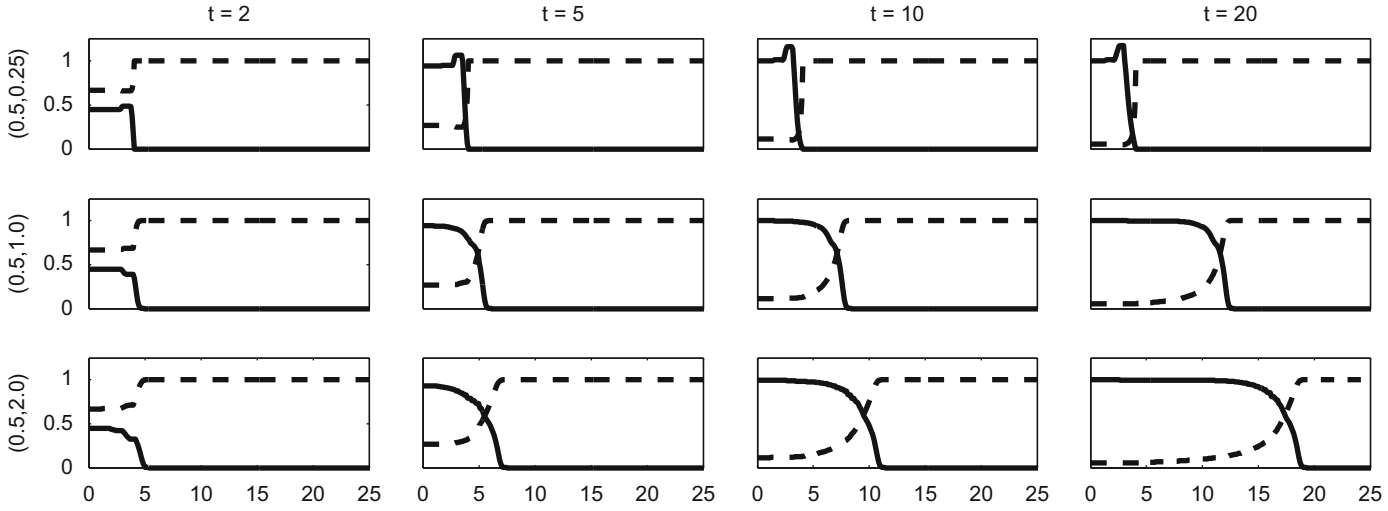

Fig. 1. Non-invasive/invasive growth depends on the cell–cell:cell–matrix adhesive strength ratio. Rows plot cell density, n, (solid) and matrix density, m (dashed line) for various (α,β) pairs: Top row, $(\alpha,\beta)=(0.5,0.25)$; Middle row, $(\alpha,\beta)=(0.5,1.0)$; Bottom row, $(\alpha,\beta)=(0.5,2.0)$. Other parameters set at $\gamma=1$, $K=2$, $m_0=1$, $n_0=0.1$, $L_i=4$ and $L=40$ (plots truncated at $x=25$ for clarity of presentation). The advection–reaction equations were solved numerically using a simplistic Method of Lines approach. Briefly, adhesive terms are discretised in conservative form via first order upwinding on a uniform mesh (with grid spacing Δx). The integral inside the advection term is calculated via direct summation. The resulting ODEs were discretised using an explicit trapezoidal scheme. We refer to Hundsdorfer and Verwer (2003) for more information on these methods. In the above simulations, we set $\Delta x = 0.1$.

Please cite this article as: Painter, K.J., et al., The impact of adhesion on cellular invasion processes in cancer and development. J. Theor. Biol. (2010), doi:10.1016/j.jtbi.2010.03.033

invasion for varying uniform initial matrix densities (in the range [0,K]) and fixed (α,β) pairs. Fig. 3(a) summarises the results. At low and medium matrix densities, invasive speed increases with matrix density. Here, the increase in matrix density combined with proteolysis creates large front-back differences in the strength of cell–matrix coupling, pulling cells forward. Yet, at higher matrix densities, the impeded movement into the tight matrix structure slows the rate of infiltration. This same trend is observed at all investigated parameter sets for which $\beta > \alpha$ (for $\alpha < \beta$, cell–cell adhesion dominates and no invasion takes place), although the maximum invasion speed clearly changes according to $\beta-\alpha$, as described in Section 3.1. We note further that at each (α,β) pair, critical matrix densities exist below/above which no invasion takes place (i.e. zero wavespeed). For larger $\beta-\alpha$, these critical values are pushed towards more extreme initial matrix densities and define locations for which the "pull-forward" of cell–matrix adhesion is counterbalanced by the "pull-back" of cell–cell adhesion: under zero cell–cell adhesion, we observe invasion for all values $\beta > 0$ and $m_0 \in (0,K)$ (see Fig. 3(a), right hand panel).

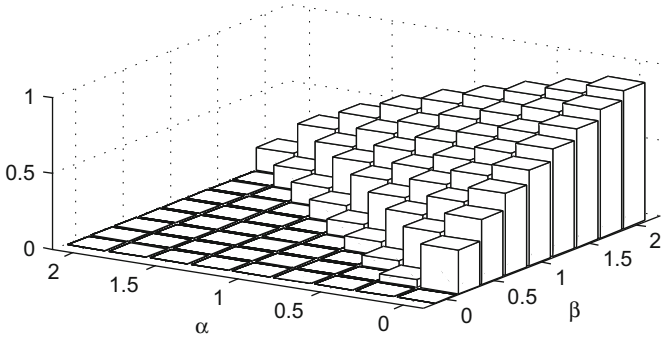

Fig. 2. Speed of invasion (indicated by height of columns) calculated for varying (α,β) pairs in the range $0 \le \alpha,\beta \le 2$. For all cases $\beta < \alpha$, no invasion takes place and the wavespeed is zero. For $\beta \ge \alpha$, invasion occurs with the speed increasing with the size of $\beta-\alpha$. Parameter and numerical details as in Fig. 1.

Expanding this further, we explore the invasion of cells into a heterogeneous ECM environment: *in vivo*, the density and structure of the ECM varies greatly both within and between tissues (e.g. see Wolf et al., 2009). To examine the impact of a heterogeneous matrix, we consider invasion of cells into the smoothly varying initial matrix distribution $m(x,0) = 0.5 + 0.5\cos(\pi x/L)$. Fig. 3(b) summarise the results from simulations conducted at three distinct (α,β) pairs. In correspondence with the results above, invasive speed varies with the position of the cell front along the x-axis and, in turn, the local matrix density. As the local matrix density drops below a critical value, invasion is halted, although the location at which this occurs depends on the magnitude of cell–matrix to cell–cell adhesion: for comparitively large cell–matrix adhesion, the cell front is able to propagate most of the way along the axis before coming to a halt. We note that similar behaviour is observed with other forms of the initial matrix density profile.

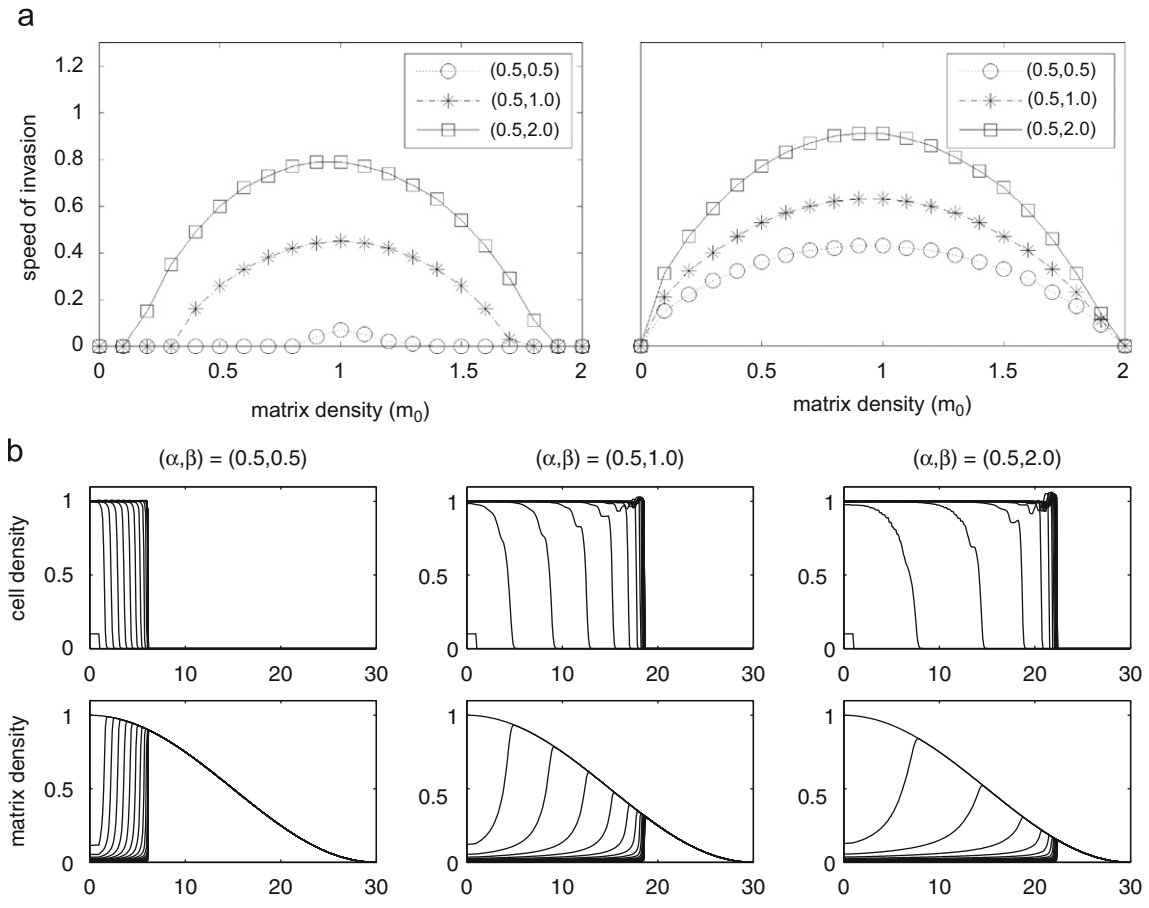

Fig. 3. Top row: wavespeeds calculated for various different initial matrix densities, m_0, and distinct (α,β) pairs: (left) wavespeeds for $\alpha = 0.5$ and $\beta = 0.5$ (dotted line/circles), $\beta = 1.0$ (dot-dash/stars) and $\beta = 2.0$ (solid/squares). (Right) wavespeeds for $\alpha = 0.0$ and $\beta = 0.5$ (dotted line/circles), $\beta = 1.0$ (dot-dash/stars) and $\beta = 2.0$ (solid/squares). Bottom row: plots showing the invasion of cells (top row) into the spatially varying matrix (bottom row), with $m(x,0) = 0.5 + 0.5\cos(\pi x/L)$. In each frame, cell/matrix densities are plotted at increments of 10 between $t = 0$ and 200. (Left) (α,β) = (0.5,0.5), (Centre) (α,β) = (0.5,1.0), (Right) (α,β) = (0.5,2.0). Other parameters are set at L=30, L_i=1.0, n_0=0.1, $\gamma = 1$, K=2.0. Numerical details as in Fig. 1. (a) Invasion speed under varying initial matrix density and (b) invasion into heterogeneous matrix.

Please cite this article as: Painter, K.J., et al., The impact of adhesion on cellular invasion processes in cancer and development. J. Theor. Biol. (2010), doi:10.1016/j.jtbi.2010.03.033

4. Exploration into the shape of the invasive interface

As described earlier, the shape of the tumour-host boundary is an important diagnostic indicator: straight/sharp boundaries generally imply noninvasive tumours while diffuse/ragged boundaries are considered hallmarks of invasiveness. Specific examples of the latter include the so-named "tumour fingers", "indian-chains" and "clusters", in which protrusions of tumour cells extend and/or break free from the main tumour mass (Friedl and Wolf, 2008). Various hypotheses have been touted for the development of such patterns, including the invasion of cells into an inhomogeneous host environment (e.g. see Anderson, 2005; Anderson et al., 2006; Gerisch and Chaplain, 2008). Nonuniform invasion is also observed during neural crest invasion. Here, time lapse imaging has revealed the formation of "streams" as the cells migrate out to pattern the peripheral nervous system (e.g. see Kulesa and Fraser, 1998; Young et al., 2004; Kasemeier-Kulesa et al., 2005). Once again, variation in the local environment is believed to play a crucial role in directing these pathways.

We use the continuous framework here to investigate in detail the role of environmental heterogeneity in regulating the shape of the invasive boundary. For computational simplicity, we restrict to a two-dimensional rectangular domain $(x,y) \in [0,L_x] \times [0,L_y]$ that describes a slice through the invasion front. Boundary conditions are as indicated in Fig. 4(a). We consider an initially quasi-1D deposition of cells adjacent to the bottom border of the domain as follows:

$$n(x,y,0) = \begin{cases} n_0 & \text{if } x \le L_i, \\ 0 & \text{otherwise.} \end{cases}$$

We note that investigations with different initial cell distributions suggest that they have relatively little impact on the general properties of the system. To determine the effect of matrix heterogeneity on invasion, we consider a variety of ECM distributions, as illustrated in Figs. 4(b)–(e):

- Alternating stripes of high/low matrix density, arranged parallel to the cell/ECM interface, $m(x,y,0) = m_0 + m_1 \cos(2\pi k_x x/L_x)$, Fig. 4(b);
- Alternating stripes of high/low matrix density, arranged perpendicular to the cell/ECM interface, $m(x,y,0) = m_0 + m_1 \cos(2\pi k_y y/L_y)$, *cf* Fig. 4(c).
- Alternating spots of low/high density, arranged in checkerboard fashion, $m(x,y,0) = m_0 + m_1 \cos(2\pi k_x x/L_x)\cos(2\pi k_y y/L_y)$, Fig. 4(d);
- randomly varying matrix, Fig. 4(e).

The time consuming nature of 2D simulations limits the capacity to perform full-scale parameter analyses and we therefore restrict our attention to a "typical" invasive parameter set, $(\alpha,\beta,\gamma,K) = (0.5,1.0,1.0,2.0)$: limited numerical simulations with other invasive parameter sets (i.e. $\beta > \alpha$) indicate qualitatively similar behaviour. For the three regular ECM distributions, Figs. 4(b)–(d), we set an average initial matrix density $m_0 = 0.5$ and classify matrix heterogeneities according to both their perturbation from m_0 (using $m_1 = 0.1,0.3,0.5$) and coarseness (or wavelength, using k_x, $k_y = 1,2$).

When the matrix is arranged in stripes running parallel to the initial cell front, we observe equivalent behaviour to the 1D investigations in Fig. 3(b). Thus, a uniform front is generated that invades into the ECM with speed changing according to the variation in matrix density along the x-axis. If the matrix density drops below the critical value, as demonstrated in Fig. 3(a), the invasion process is halted.

However, for stripes arranged perpendicularly to the initial cell front, matrix density varies with position along the front. As such, the speed of invasion varies and the result is growing "fingers" that project out along the lines of higher initial matrix density (Fig. 5) with the thickness of the projections correlating with the wavelength of the imposed matrix variation. If the matrix density drops to sufficiently low values, no invasion occurs into those areas. For an initial checkerboard-style matrix as in Fig. 4(d), we also observe nonuniform invasion into the matrix, although fingers will now expand and shrink to reflect the locally varying matrix density (Fig. 6). Once again, no invasion takes place into areas in which the matrix density is sufficiently low, leaving non-occupied "holes" as the cell population expands. These results reveal a critical relationship between the form of the invasive front and the local ECM structure.

We conclude this investigation by exploring the impact of more realistic, randomised initial matrix densities (as illustrated in Fig. 4(e)). The timecourse of one such simulation is plotted in Fig. 7, revealing a highly variable invasion front that changes considerably over both space and time: for example, by $t = 50$ we see that some parts of the tumour front have invaded about twice as far as others. We note that the degree of this variation is transient, depending strongly on the specific matrix heterogeneity.

To explore how distinct measures of matrix heterogeneity differentially impact on the front, we consider invasion into random initial matrix that varies with respect to both perturbation from the mean level ($m_0 = 0.5$) and its coarseness (i.e. the average wavelength in the initial heterogeneity). Fig. 8 plots the calculated cell distributions at $t = 40$. Our simulations indicate that both

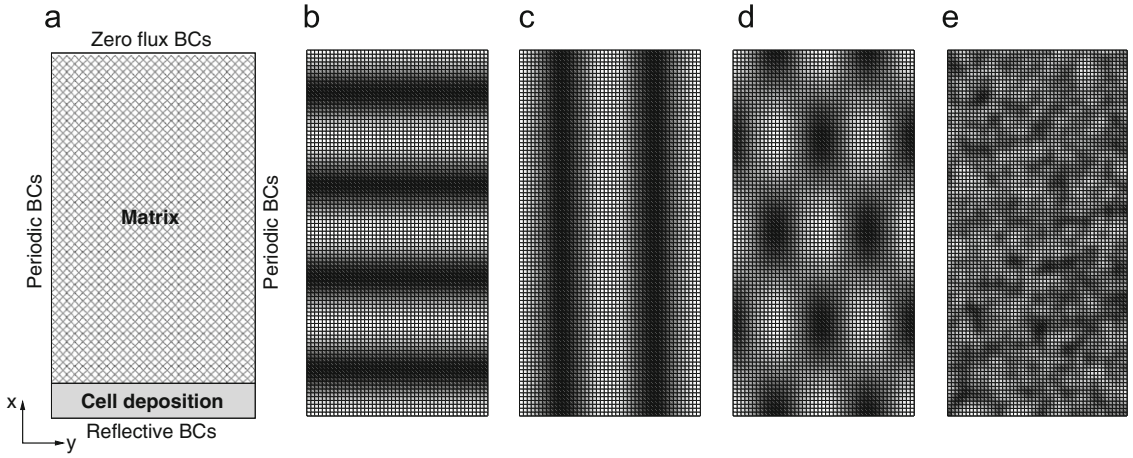

Fig. 4. (a) Schematic showing the set-up for the 2D invasion model. Cells are deposited within a narrow strip adjacent to the $x = 0$ boundary. Surrounding region (cross-hatched area) contains matrix only, with the initially imposed matrix heterogeneity varying according to the forms described in (b)–(e) (see text for further details).

Please cite this article as: Painter, K.J., et al., The impact of adhesion on cellular invasion processes in cancer and development. J. Theor. Biol. (2010), doi:10.1016/j.jtbi.2010.03.033

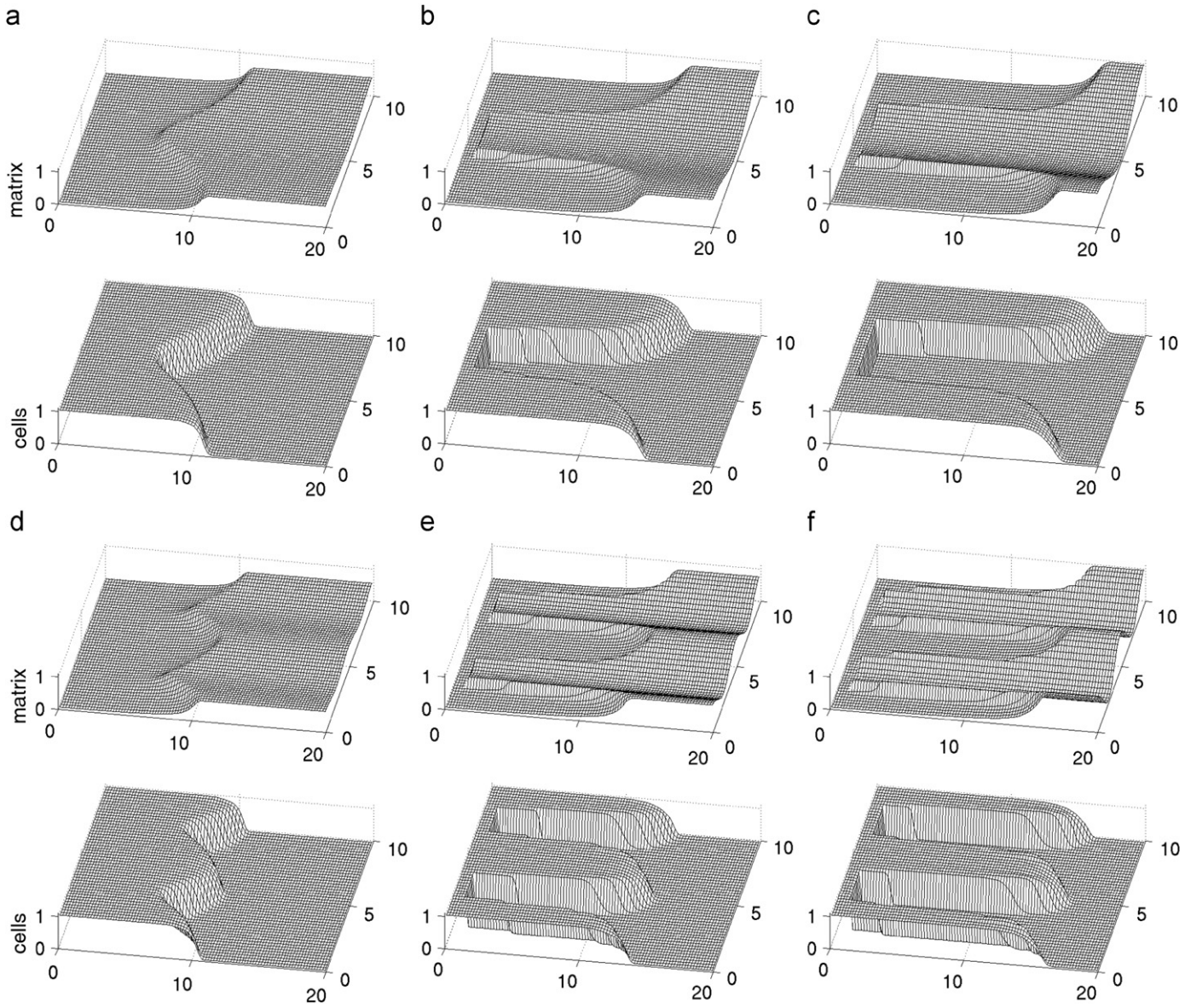

Fig. 5. "Fingers" generated through invasion of cells into an initial matrix in which matrix density varies along the invasion front. For each subfigure (a)–(f), plots represent matrix density (top) and cell density (bottom) plotted on the rectangular domain $(x,y) \in [0,20] \times [0,10]$ at the fixed time $t=40$ for the following initial matrix distributions: (a) $m_0=0.5$, $m_1=0.1$, $k_y=1$; (b) $m_0=0.5$, $m_1=0.3$, $k_y=1$; (c) $m_0=0.5$, $m_1=0.5$, $k_y=1$; (d) $m_0=0.5$, $m_1=0.1$, $k_y=2$; (e) $m_0=0.5$, $m_1=0.3$, $k_y=2$; (f) $m_0=0.5$, $m_1=0.5$, $k_y=2$. Model parameters are set as described in the text, $(\alpha,\beta,\gamma,K)=(0.5,1.0,1.0,2.0)$, with $n_0=0.1$ and $L_i=1$. The 2D model was solved numerically in conservative form using a method of lines approach similar to that described for the 1D numerics, with the 2D domain discretised onto a uniform grid of spacing $\Delta x=\Delta y=0.2$. The advective component is approximated via first order upwinding, with the 2D integral inside the advective term approximated as described in Armstrong et al. (2009). We note that a number of more efficient numerical methods have been developed for systems similar to (4), see Gerisch and Chaplain (2008), Gerisch and Painter (2010), and Gerisch (2010) for details, although such schemes would require–modification for the boundary conditions specified here.

factors are critical for generating heterogeneous invasion fronts. Under relatively low perturbations (left-most columns), any variation in the invasion speed along the y-axis is minimal and the front is relatively smooth in nature. Increasing the perturbations (left to right columns) leads to greater variations in invasion speed and correspondingly, a more jagged front. Note that "holes" can be observed if the matrix density drops to critically low levels in a sufficiently large pocket of matrix. Similar observations derive from an investigation into the impact of matrix coarseness on the front: for finely varying matrix (i.e. low wavelength/coarseness) (Fig. 8, top row), any variation in the matrix is of shorter wavelength than the sensing radius of cells and the integral effectively smooths out this heterogeneity. The subsequent invasion takes place with a more or less uniform front. Increasing the coarseness (top to bottom rows) results in greater differences in the invasive speed and correspondingly, a more variable tumour front.

5. Discussion

In the course of this paper we have expanded on our earlier continuous-level modelling (e.g. see Armstrong et al., 2006; Sherratt et al., 2009; Gerisch and Painter, 2010) to develop a relatively simple model for studying cellular invasion that incorporates cell–cell adhesion, cell–matrix adhesion and proteolytic degradation of a surrounding extracellular matrix. Under sufficiently strong cell–matrix adhesion and/or sufficiently weak cell–cell adhesion, we observe the expansion of a cell population as it degrades and invades the surrounding ECM environment.

Please cite this article as: Painter, K.J., et al., The impact of adhesion on cellular invasion processes in cancer and development. J. Theor. Biol. (2010), doi:10.1016/j.jtbi.2010.03.033

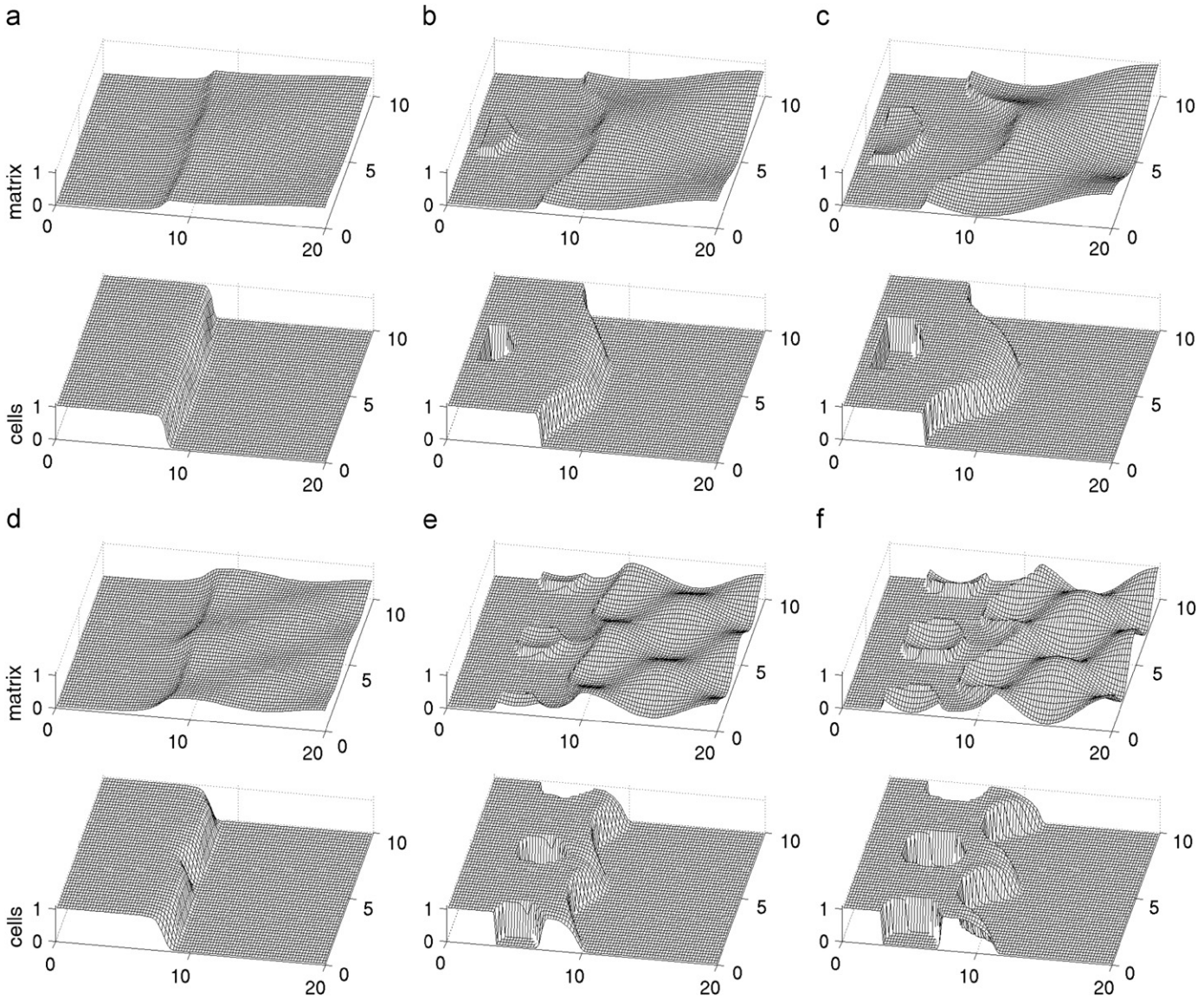

Fig. 6. Invasion of cells into a "checkerboard" matrix. For each subfigure (a)–(f), plots represent matrix density (top) and cell density (bottom) plotted on the rectangular domain $(x,y) \in [0,20] \times [0,10]$ at the fixed time $t=40$ for the following initial matrix distributions: (a) $m_0=0.5$, $m_1=0.1$, $k_y=k_x=1$; (b) $m_0=0.5$, $m_1=0.3$, $k_y=k_x=1$; (c) $m_0=0.5$, $m_1=0.5$, $k_y=k_x=1$; (d) $m_0=0.5$, $m_1=0.1$, $k_y=k_x=2$; (e) $m_0=0.5$, $m_1=0.3$, $k_y=k_x=2$; (f) $m_0=0.5$, $m_1=0.5$, $k_y=k_x=2$. Other model details as for Fig. 5.

The structure and heterogeneity of the matrix plays a significant role in shaping the dynamics: highly heterogeneous and variable ECM can lead to "fingering" at the invasive front. These results echo similar findings by others in both hybrid discrete-continuous (e.g. Anderson, 2005; Anderson et al., 2006) and fully continuous models (e.g. Gerisch and Chaplain, 2008). Significantly, under confocal microscopy techniques Wolf et al. (2009) reveal that within the same tissue, *in vivo* collagen scaffolds cover a range between low and high density networks with highly variable pore size. Note that for a sufficiently homogeneous matrix, our model predicts that invasion can occur with a smooth front (Fig. 8 top rows): invasion is not necessarily synonymous with a jagged appearance of the front.

In its current form, the model is intentionally simplistic to facilitate an initial study into the impact of adhesion and matrix degradation on the form of invasion. As such, the present results are qualitative rather than quantitative and a number of further extensions to the model would be required before applying it to specific systems. For example, the manner in which cells interact with the matrix is significantly more complex than in the toy model described here. We note that a number of authors have developed more detailed models to describe cell–matrix interactions (e.g. Chaplain and Lolas, 2005; Mallet and Pettet, 2006; MacArthur et al., 2005; Gerisch and Chaplain, 2008) and it would be of interest to examine how they can be incorporated and extended within the current framework. For example, certain environmental factors are known to modulate multiple processes associated with invasion and the incorporation of this detail within the model may provide insight into ambiguities associated with their capacity to facilitate or impede invasion.

The live imaging of migrating cells *in vivo* indicates that proteolysis is a highly focussed process, capable of significantly reordering matrix alignment. Proteolysis at the front of the cell is accompanied by the remodelling of matrix fibres at the rear to create a locally aligned trail of fibres along the path of cell migration (e.g. Friedl and Wolf, 2009). Such trails may provide a guidance cue to the cells (contact guidance) and detailed modelling by a number of authors using both discrete (e.g. Dallon et al., 1999; McDougall et al., 2006) and continuous approaches (e.g. Dallon and Sherratt, 2000; Hillen, 2006; Painter, 2009)

Please cite this article as: Painter, K.J., et al., The impact of adhesion on cellular invasion processes in cancer and development. J. Theor. Biol. (2010), doi:10.1016/j.jtbi.2010.03.033

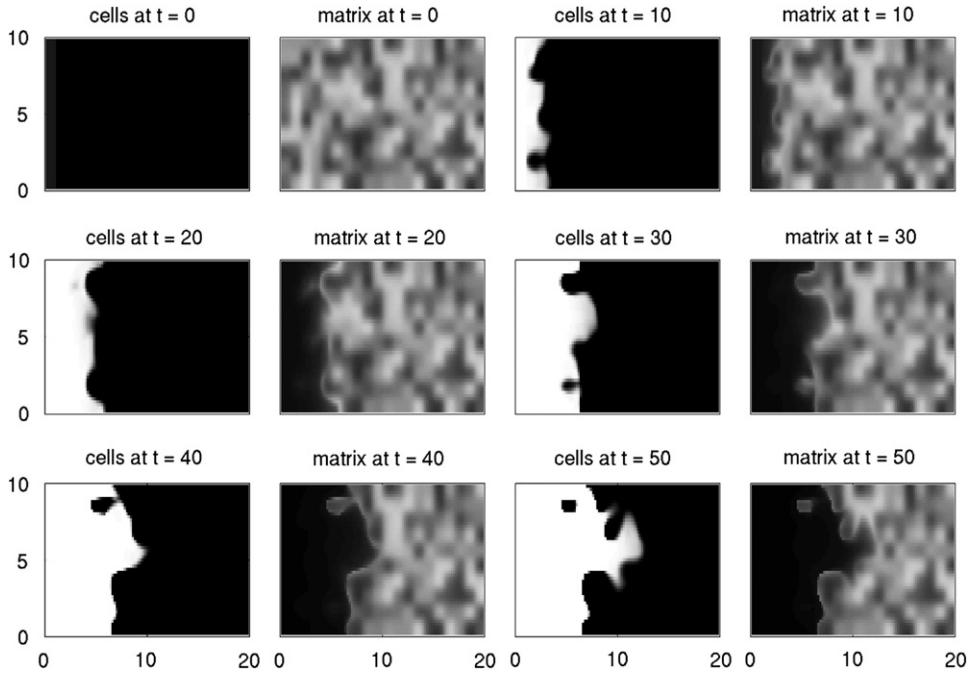

Fig. 7. Time evolution of a cell invasion front into a "randomised" matrix structure. Cell (n) and matrix (m) densities are plotted at the various times shown, using a grayscale indicator (black indicating zero density and white representing a density of 1). Other model details as for Fig. 5.

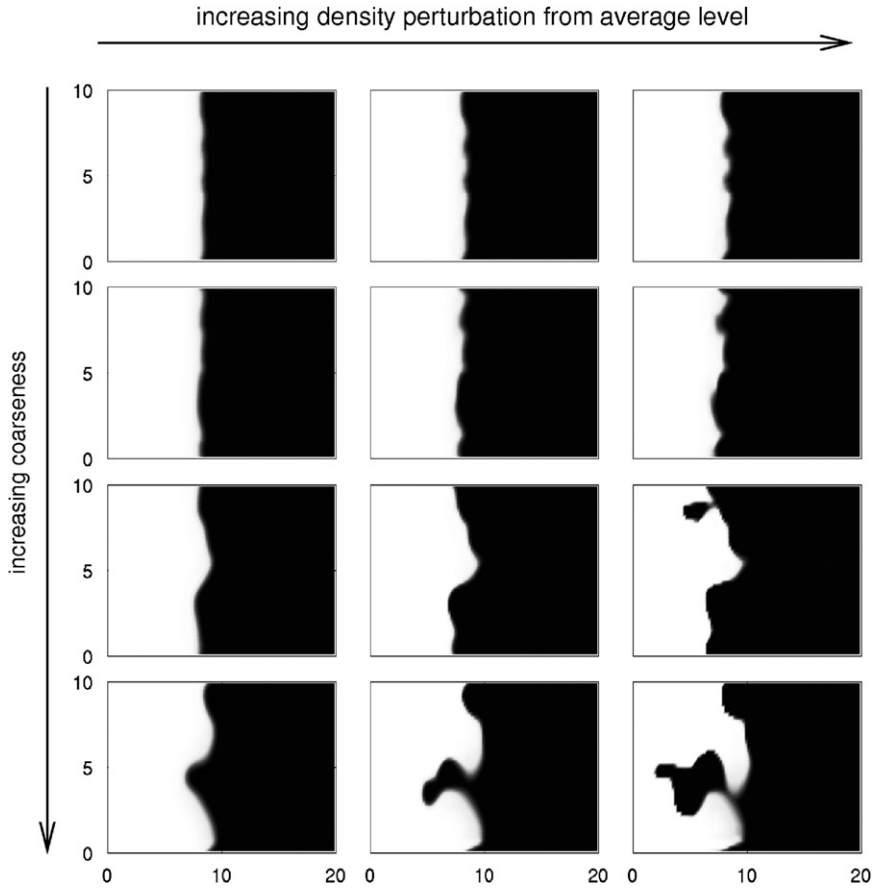

Fig. 8. Cell invasion into various randomised initial matrices. Cell distributions plotted at $t=40$ as density maps (white representing a density of 1, black representing a density of zero). Other model details as for Fig. 5.

indicate that it forms a powerful mechanism for generating "cellular highways", i.e. paths in the matrix along which cells preferentially migrate. An interesting exploration would be to investigate whether the addition of adhesive interactions within such models either enhances or diminishes the capacity of cells to generate heterogeneous patterns of invasion.

Please cite this article as: Painter, K.J., et al., The impact of adhesion on cellular invasion processes in cancer and development. J. Theor. Biol. (2010), doi:10.1016/j.jtbi.2010.03.033

The focus of our work has been on the invasive properties of a single cell population, exploring how its specific adhesive properties alter its capacity to invade. In reference to tumour growth, therefore, the framework here is most suitably applied to the *in vitro* deposition of specific cell lines within a suitable collagen matrix (e.g. Tranquillo, 1999; Shreiber et al., 2003; Baba et al., 2004). *In vivo*, tumour growth occurs within a far more complicated environment: for example, a tumour may develop within a surrounding healthy population while the surrounding matrix will also include a variety of other cell types (e.g. fibroblasts). Interactions between tumour cells and healthy cells have previously been modelled within a reaction–diffusion framework (e.g. Sherratt and Nowak, 1992; Gatenby, 1995; Sherratt and Chaplain, 2001; Painter and Sherratt, 2003; Smallbone et al., 2008), and our model provides a way of including the potential adhesive interactions between the tumour and healthy cells in such studies. In a similar vein, another potential extension of the model would be to explore pathways to malignancy via the addition of mutated subpopulations with distinct adhesive, proteolytic and proliferative properties. Differential adhesion in distinct cell types is a powerful mechanism for the patterning of cell populations, a process known as cell sorting (e.g. Foty and Steinberg, 2004; Steinberg, 2007) and it would be of interest to determine how such processes contribute to the rearrangement and invasion of tumours.

The application to neural crest cell invasion is another area for consideration. Following their emergence along the dorsal neural tube, neural crest cells migrate away to pattern various structures including components of the peripheral nervous system. Migration occurs in a highly structured fashion, with cells following stereotypical pathways and often forming collective "streams" and "chains" (Kulesa and Fraser, 1998; Young et al., 2004; Kasemeier-Kulesa et al., 2005) through a combination of signals within the neural tube, cell–cell contacts, and spatial variation in the extracellular distribution of attractive and repulsive cues (e.g. Young et al., 2004; Kasemeier-Kulesa et al., 2008). Our framework, while currently focusing on attractive/adhesive interactions, could easily be adapted to add additional processes such as repulsion to investigate their contribution to the invasive process.

Acknowledgements

NJA was supported by a Doctoral Training Account Studentship from EPSRC. KJP and JAS were supported in part by Integrative Cancer Biology Program Grant CA113004 from the US National Institutes of Health and in part by BBSRC grant BB/D019621/1 for the Centre for Systems Biology at Edinburgh. JAS was also supported in part by a Leverhulme Trust Research Fellowship.

References

Abu-Eid, R., Landini, G., 2006. Morphometrical differences between pseudoepitheliomatous hyperplasia in granular cell tumours and squamous cell carcinomas. Histopathology 48, 407–416.
Anderson, A.R.A., 2005. A hybrid model of solid tumour invasion: the importance of cell adhesion. Math. Med. Biol. 22, 163–186.
Anderson, A.R.A., Rejniak, K.A., Gerlee, P., Quaranta, V., 2009. Microenvironment driven invasion: a multiscale multimodel investigation. J. Math. Biol. 58, 579–624.
Anderson, A.R.A., Weaver, A.M., Cummings, P.T., Quaranta, V., 2006. Tumor morphology and phenotypic evolution driven by selective pressure from the microenvironment. Cell 127, 905–915.
Armstrong, N.J., Painter, K.J., Sherratt, J.A., 2006. A continuum approach to modelling cell–cell adhesion. J. Theor. Biol. 243, 98–113.
Armstrong, N.J., Painter, K.J., Sherratt, J.A., 2009. Adding adhesion to a chemical signaling model for somite formation. Bull. Math. Biol. 71, 1–24.
Baba, M., Itoh, K., Tatsuta, M., 2004. Glycine-extended gastrin induces matrix metalloproteinase-1-and-3-mediated invasion of human colon cancer cells through type I collagen gel and matrigel. Int. J. Cancer 111, 23–31.
Berrier, A.L., Yamada, K.M., 2007. Cell–matrix adhesion. J. Cell. Physiol. 213, 565–573.
Byrne, H.M., Chaplain, M.A.J., 1996. Modelling the role of cell–cell adhesion in the growth and development of carcinomas. Math. Comp. Modelling 24, 1–17.
Cavallaro, U., Christofori, G., 2004. Cell adhesion and signalling by cadherins and Ig-CAMs in cancer. Nat. Rev. Cancer 4, 118–132.
Chaplain, M.A.J., 1996. Avascular growth, angiogenesis and vascular growth in solid tumours: the mathematical modelling of the stages of tumour development. Math. Comp. Modelling 23, 47–87.
Chaplain, M.A.J., Lolas, G., 2005. Mathematical modelling of cancer cell invasion of tissue: the role of the urokinase plasminogen activation system. Math. Mod. Meth. Appl. Sci. 15, 1685–1734.
Christofori, G., 2003. Changing neighbours, changing behaviour: cell adhesion molecule-mediated signalling during tumour progression. EMBO J. 22, 2318–2323.
Cristini, V., Lowengrub, J., Nie, Q., 2003. Nonlinear simulation of tumour growth. Math. Biol. 46, 191–224.
Dallon, J.C., Sherratt, J.A., 2000. A mathematical model for spatially varying extracellular alignment. SIAM J. Appl. Math. 61 (2), 506–527.
Dallon, J.C., Sherratt, J.A., Maini, P.K., 1999. Mathematical modelling of extracellular matrix dynamics using discrete cells: fiber orientation and tissue regeneration. J. Theor. Biol. 199, 449–471.
Dunn, G., Heath, J.P., 1976. New hypothesis of contact guidance in tissue–cells. Exp. Cell. Res. 101, 1–14.
Foty, R.A., Steinberg, M.S., 2004. Cadherin-mediated cell–cell adhesion and tissue segregation in relation to malignancy. Int. J. Dev. Biol. 48, 397–409.
Frieboes, H.B., Lowengrub, J.S., Wise, S., Zheng, X., Macklin, P., Bearer, E.L., Cristini, V., 2007. Computer simulation of glioma growth and morphology. Neuroimage 37 (Suppl. 1), 59–70.
Frieboes, H.B., Zheng, X., Sun, C.H., Tromberg, B., Gatenby, R., Cristini, V., 2006. An integrated computational/experimental model of tumor invasion. Cancer Res. 66, 1597–1604.
Friedl, P., Gilmour, D., 2009. Collective cell migration in morphogenesis, regeneration and cancer. Nat. Rev. Mol. Cell Biol. 10, 445–457.
Friedl, P., Wolf, K., 2003. Tumour–cell invasion and migration: diversity and escape mechanisms. Nat. Rev. Cancer 3, 362–374.
Friedl, P., Wolf, K., 2008. Tube travel: the role of proteases in individual and collective cancer cell invasion. Cancer Res. 68, 7247–7249.
Friedl, P., Wolf, K., 2009. Proteolytic interstitial cell migration: a five-step process. Cancer Metastasis Rev. 28, 129–135.
Friedman, A., 2007. Mathematical analysis and challenges arising from models of tumor growth. Math. Mod. Meth. Appl. Sci. 17, 1751–1772.
Gatenby, R.A., 1995. Models of tumor-host interaction as competing populations: implications for tumor biology and treatment. J. Theor. Biol. 176, 447–455.
Gerisch, A., 2010. On the approximation and efficient evaluation of integral terms in PDE models of cell adhesion. IMA J. Numer. Anal. 30, 173–194.
Gerisch, A., Chaplain, M.A.J., 2008. Mathematical modelling of cancer cell invasion of tissue: local and non-local models and the effect of adhesion. J. Theor. Biol. 250, 684–704.
Gerisch, A., Painter, K.J., 2010. Cell Mechanics: From Single Scale Based Models to Multiscale Modeling Mathematical Modelling of Cell Adhesion and its Applications to Developmental Biology and Cancer Invasion. Taylor and Francis, London (Chapter 12).
Grygierzec, W., Deutsch, A., Philipsen, L., Friedenberger, M., Schubert, W., 2004. Modelling tumour cell population dynamics based on molecular adhesion assumptions. J. Biol. Syst. 12, 273–288.
Hillen, T., 2006. M5 mesoscopic and macroscopic models for mesenchymal motion. J. Math. Biol. 53, 585–616.
Hundsdorfer, W., Verwer, J.G., 2003. Numerical Solution of Time-Dependent Advection-Diffusion–Reaction Equations. Springer Series in Computational Mathematics, vol. 33, Springer.
Kasemeier-Kulesa, J.C., Kulesa, P.M., Lefcort, F., 2005. Imaging neural crest cell dynamics during formation of dorsal root ganglia and sympathetic ganglia. Development 132, 235–245.
Kasemeier-Kulesa, J.C., Teddy, J.M., Postovit, L.M., Seftor, E.A., Seftor, R.E., Hendrix, M.J., Kulesa, P.M., 2008. Reprogramming multipotent tumor cells with the embryonic neural crest microenvironment. Dev. Dyn. 237, 2657–2666.
Kim, Y., Lawler, S., Nowicki, M.O., Chiocca, E.A., Friedman, A., 2009. A mathematical model for pattern formation of glioma cells outside the tumor spheroid core. J. Theor. Biol. 260, 359–371.
Kulesa, P.M., Fraser, S.E., 1998. Neural crest cell dynamics revealed by time-lapse video microscopy of whole embryo chick explant cultures. Dev. Biol. 204, 327–344.
Landini, G., Rippin, J.W., 1996. How important is tumour shape? Quantification of the epithelial-connective tissue interface in oral lesions using local connected fractal dimension analysis. J. Pathol. 179, 210–217.
Landman, K.A., Simpson, M.J., Pettet, G.J., 2008. Tactically-driven nonmonotone travelling waves. Physica D 237, 678–691.
Lo, L.M., Wang, H.B., Dembo, M., Wang, Y.L., 2000. Cell movement is guided by the rigidity of the substrate. Biophys. J. 79, 144–152.
MacArthur, B.D., Please, C.P., Pettet, G.J., 2005. A mathematical model of dynamic glioma–host interactions: receptor-mediated invasion and local proteolysis. Math. Med. Biol. 22, 247–264.
Macklin, P., Lowengrub, J., 2007. Nonlinear simulation of the effect of microenvironment on tumor growth. J. Theor. Biol. 245, 677–704.
Mallet, D., Pettet, G., 2006. A mathematical model of integrin-mediated haptotactic cell migration. Bull. Math. Biol. 68, 231–253.
Manwaring, M.E., Walsh, J.F., Tresco, P.A., 2004. Contact guidance induced organization of extracellular matrix. Biomaterials 25, 3631–3638.

Please cite this article as: Painter, K.J., et al., The impact of adhesion on cellular invasion processes in cancer and development. J. Theor. Biol. (2010), doi:10.1016/j.jtbi.2010.03.033

Marchant, B.P., Norbury, J., Sherratt, J.A., 2001. Travelling wave solutions to a haptotaxis-dominated model of malignant invasion. Nonlinearity 14, 1653–1671.

McDougall, S., Dallon, J., Sherratt, J.A., Maini, P., 2006. Fibroblast migration and collagen deposition during dermal wound healing: mathematical modelling and clinical implications. Philos. Trans. A. Math. Phys. Eng. Sci. 364, 1385–1405.

Mignatti, P., Rifkin, D.B., 1993. Biology and biochemistry of proteinases in tumour invasion. Physiol. Rev. 73, 161–195.

Nieto, M.A., 2009. Epithelial–mesenchymal transitions in development and disease: old views and new perspectives. Int. J. Dev. Biol. 53, 1541–1547.

Painter, K.J., 2009. Modelling cell migration strategies in the extracellular matrix. J. Math. Biol. 58, 511–543.

Painter, K.J., Sherratt, J.A., 2003. Modelling the movement of interacting cell populations. J. Theor. Biol. 225, 327–339.

Perumpanani, A.J., Sherratt, J.A., Norbury, J., Byrne, H.M., 1996. Biological inferences from a mathematical model for malignant invasion. Invasion and Metastasis 16, 209–221.

Poplawski, N.J., Agero, U., Gens, J.S., Swat, M., Glazier, J.A., Anderson, A.R.A., 2009. Front instabilities and invasiveness of simulated avascular tumors. Bull. Math. Biol. 71, 1189–1227.

Ramis-Conde, I., Drasdo, D., Anderson, A.R.A., Chaplain, M.A.J., 2008. Modeling the influence of the E-cadherin-beta-catenin pathway in cancer cell invasion: a multiscale approach. Biophys. J. 95, 155–165.

Sekimura, T., Zhu, M., Cook, J., Maini, P., Murray, J., 1999. Pattern formation of scale cells in lepidoptera by differential origin-dependent cell adhesion. Bull. Math. Biol. 61, 807–827.

Sherratt, J.A., Chaplain, M.A.J., 2001. A new mathematical model for avascular tumour growth. J. Math. Biol. 43, 291–312.

Sherratt, J.A., Gourley, S., Armstrong, N.A., Painter, K.J., 2009. Boundedness of solutions of a non-local reaction–diffusion model for adhesion in cell aggregation and cancer invasion. Eur. J. Appl. Math. 20, 123–144.

Sherratt, J.A., Nowak, M.A., 1992. Oncogenes, anti-oncogenes and the immune response to cancer. Proc. R. Soc. London B 248, 261–272.

Shreiber, D.I., Barocas, V.H., Tranquillo, R.T., 2003. Temporal variations in cell migration and traction during fibroblast-mediated gel compaction. Biophys. J. 84, 4102–4114.

Smallbone, K., Gatenby, R.A., Maini, P.K., 2008. Mathematical modelling of tumour acidity. J. Theor. Biol. 255, 106–112.

Steinberg, M.S., 2007. Differential adhesion in morphogenesis: a modern view. Curr. Opin. Genet. Dev. 17, 281–286.

Szymanska, Z., Morales Rodrigo, C., Lachowicz, M., Chaplain, M., 2009. Mathematical modelling of cancer invasion of tissue: the role and effect of nonlocal interactions. Math. Mod. Meth. Appl. Sci. 19, 257–281.

Tranquillo, R.T., 1999. Self-organization of tissue-equivalents: the nature and role of contact guidance. Biochem. Soc. Symp. 65, 27–42.

Turner, S., Sherratt, J.A., 2002. Intercellular adhesion and cancer invasion: a discrete simulation using the extended Potts model. J. Theor. Biol. 216, 85–100.

Turner, S., Sherratt, J.A., Painter, K.J., Savill, N.J., 2004. From a discrete to a continuous model of biological cell movement. Phys. Rev. E 69, 021910.

Wheelock, M.J., Shintani, Y., Maeda, M., Fukumoto, Y., Johnson, K., 2008. Cadherin switching. J. Cell. Sci. 121, 727–735.

Wolf, K., Alexander, S., Schacht, V., Coussens, L.M., von Andrian, U.H., van Rheenen, J., Deryugina, E., Friedl, P., 2009. Collagen-based cell migration models in vitro and in vivo. Semin. Cell Dev. Biol. 20, 931–941.

Yilmaz, M., Christofori, G., 2009. EMT, the cytoskeleton, and cancer cell invasion. Cancer Metastasis Rev. 28, 15–33.

Yilmaz, M., Christofori, G., Lehembre, F., 2007. Distinct mechanisms of tumor invasion and metastasis. Trends Mol. Med. 13, 535–541.

Young, H.M., Bergner, A.J., Anderson, R.B., Enomoto, H., Milbrandt, J., Newgreen, D.F., Whitington, P.M., 2004. Dynamics of neural crest-derived cell migration in the embryonic mouse gut. Dev. Biol. 270, 455–473.

Please cite this article as: Painter, K.J., et al., The impact of adhesion on cellular invasion processes in cancer and development. J. Theor. Biol. (2010), doi:10.1016/j.jtbi.2010.03.033